Thieme

Relaxed Alert Electroencephalography Screening for Mild Traumatic Brain Injury in Athletes

Authors
Samah Abdul Baki[1], Zohreh Zakeri[2], Geetha Chari[3], André Fenton[4], Ahmet Omurtag[2]

Affiliations
1 Clinical BioSignal Group Corp., Acton, Massachusetts, United States
2 Department of Engineering, Nottingham Trent University School of Science and Technology, Nottingham, United Kingdom of Great Britain and Northern Ireland
3 Pediatric Neurology, SUNY Downstate Medical Center, New York City, United States
4 Center for Neural Science, NYU, New York, United States

Key words
mild traumatic brain injury, EEG, phase locking value

accepted 10.05.2023
published online 25.07.2023

Bibliography
Int J Sports Med 2023; 44: 896–905
DOI 10.1055/a-2091-4860
ISSN 0172-4622

Georg Thieme Verlag, Rüdigerstraße 14,
70469 Stuttgart, Germany

Correspondence
Dr. Samah Abdul Baki
BioSignal Group Corp.
Clinical, 3 post office square
01720 Acton, Massachusetts
United States
Tel.: +1-3473460729, Fax: 844-429-8293
sbaki@biosignalgroup.com

ABSTRACT

Due to the mildness of initial injury, many athletes with recurrent mild traumatic brain injury (mTBI) are misdiagnosed with other neuropsychiatric illnesses. This study was designed as a proof-of-principle feasibility trial for athletic trainers at a sports facility to generate electroencephalograms (EEGs) from student athletes for discriminating (mTBI) associated EEGs from uninjured ones. A total of 47 EEGs were generated, with 30 athletes recruited at baseline (BL) pre-season, after a concussive injury (IN), and post-season (PS). Outcomes included: 1) visual analyses of EEGs by a neurologist; 2) support vector machine (SVM) classification for inferences about whether particular groups belonged to the three subgroups of BL, IN, or PS; and 3) analyses of EEG synchronies including phase locking value (PLV) computed between pairs of distinct electrodes. All EEGs were visually interpreted as normal. SVM classification showed that BL and IN could be discriminated with 81 % accuracy using features of EEG synchronies combined. Frontal interhemispheric phase synchronization measured by PLV was significantly lower in the IN group. It is feasible for athletic trainers to record high quality EEGs from student athletes. Also, spatially localized metrics of EEG synchrony can discriminate mTBI associated EEGs from control EEGs.

Introduction

Traumatic brain injury (TBI) is defined as "an alteration in brain function or other evidence of brain pathology, caused by an external force [1]." It may be caused by accidents and violence, and accounts for one-third of all injury-related deaths in the United States. About 3 % of the population experience chronic disability related to TBI. It is associated with a broad spectrum of symptoms that unfold over hours to months and, in some cases, indefinitely. Mild TBI (mTBI) patients constitute a large majority of all recorded cases of TBI [2–4]. Although most mTBI patients recover, a substantial minority (7–33 %) develop persistent disabilities (post-concussive syndrome or PCS) in the form of somatic (headaches, dizziness), cognitive (attention and memory impairment), and emotional (irritability, depression) problems [5]. The diagnosis of mTBI is difficult and exacerbated by the fact that individual patients experience different subsets of clinical symptoms. Cumulative effects of multiple concussions demonstrate that latent dysfunction lingers even in patients whose symptoms have resolved. Reports suggest that 11–23 % of deployed service members have mTBI [6].

Brain imaging technologies have been used to assess mTBI, and because computed tomography (CT) is practical and ubiquitous in emergency medicine, CT is commonly the first neuroimaging pro-

cedure to be used for the mTBI patient. However, CT findings or other structural imaging have been poor predictors of long-term sequelae, perhaps because mTBI is not associated with bleeding or other gross trauma, unlike more severe brain injuries [7, 8]. This is partly due to the fact that mTBI injuries are primarily microscopic and diffuse and most mTBI patients have normal CT and structural magnetic resonance imaging (MRI) scans [9, 10]. Diffusion tensor imaging (DTI), another structural assessment, could not discriminate between normal and mTBI patients even when the patients had post-concussive symptoms such as verbal memory deficits [11]. Although more recent DTI efforts have had some success in distinguishing mTBI and control patients, mTBI appears to impact brain function to a greater extent than it impacts brain structure [12].

Concussion is common and physicians face serious challenges in the management and prognostication of mTBI. In the US, emergency departments (EDs) receive 1.2 million patients with TBI, accounting for 1.2 % of all ED visits, with 38 % of these patients being discharged home without specific recommendations for follow-up [2, 13, 14]. In a longitudinal study of mTBI patients presenting to the ED, 82 % of patients reported at least one subsequent post-concussive symptom and > 40 % had significantly reduced Satisfaction with Life scores post-injury, indicating mTBI produces significant disability [4].

Sports-related concussion is one of the major causes of TBI and increasing media coverage of professional athletes whose careers were ended by brain injury and recent relevant changes to the National Football League policy reflect only one aspect of the overall societal impact of mTBI [15–17].

High school football players had alterations in default mode network (DMN) activation measured by fMRI functional covariance as compared to non-contact sports athletes [18]. Significant reductions in DMN activation of football players were shown at 7 days after injury [19]. Significant cerebral glucose metabolism changes were found in former National Football League players who had suffered repetitive sub-concussive injury as well as concussions during their careers [20]. Many athletes with no single mTBI event may accumulate thousands of sub-concussive incidents eventually resulting in neurological impairment [21]. In athletes with sports-related injuries, EEG abnormalities extracted by analysis persisted after the post-concussive symptoms had resolved, suggesting that EEG can be useful to detect and manage mTBI [22, 23].

Could EEG be used to manage mTBI in athletes? For EEG to be practical in managing sports concussion, it should be easy to record high-quality, clinical-grade EEG at sports facilities, and quantitative measures from the EEG should be sufficient to accurately distinguish between injury and non-injury EEGs. Resting-state EEG requires that the subject sit or lie still, making it a promising methodology for determining the presence and severity of mTBI. Resting-state recordings are easy for the subjects as well as for the EEG operator to collect, because no motor, cognitive, or other neurological tests are administered. In the present study, EEGs were recorded at a university sports facility by athletic trainers so we could assess whether it is practical and convenient to collect high-quality EEGs from athletes. We used commercially available systems, microEEG, a portable, wireless battery-operated amplifier device as well as StatNet, a rapid-to-apply, single-use disposable EEG electrode cap. A resting-state EEG was collected from college athletes at baseline (BL) before the sports season, after a concussive injury (IN), and post-season (PS). Analysis of the recordings by extracting quantitative measures of local and inter-area neural activity synchronization and binary injury/non-injury classification demonstrates that the EEGs could be discriminated with 81 % accuracy. By examining the individual quantitative features extracted from the EEG, we find that inter-hemispheric phase synchronization is significantly lower in the Injury group.

Materials and Methods

Participants, data collection, and study design

A total of 15 female and 15 male subjects participated; each was a member of a collegiate sports team at Massachusetts Institute of Technology (MIT) and consented to participate according to IRB and NIH guidelines. In general, the study was conducted in conformity with the declaration of Helsinki and Good Clinical Practice [24]. Resting-state EEG was recorded in the sports facility by athletic trainers who had previously learned to use the equipment and administer the EEG during a 5-hour training session. The training duration for the athletic trainers was up to five hours, which included the vetting process of their EEG readouts prior to authorizing them to record EEG signals from the athletes.

A minimum of 15-min resting-state EEG with eyes closed was recorded while the subject sat in a chair. EEGs were recorded using StatNet, a single-use disposable system of 16 electrodes that takes less than 5 minutes to apply to the subject [25]. The StatNet was connected to microEEG, a portable, battery-operated, wireless, digital EEG recording system [26, 27]. The data were stored on a hard disk for offline clinical review by a board-certified neurologist, as well as separate quantitative analysis using digital signal processing techniques that are detailed next.

Data analysis

The digital signal processing and calculations described in this paper used Matlab v.9.3.0.713579 (The MathWorks, Inc., Natick, Massachusetts, United States).

Pre-processing

The raw EEG was first pre-processed to minimize or eliminate signal artefacts originating from outside the brain. Initially the recordings were visually inspected in the frequency and time domains. The power spectra of all the recordings contained an alpha rhythm peak (8–12 Hz), especially in the parietal and occipital areas, and the amounts of relative power in any frequency bands contained no gross inconsistency relative to expectations [27]. The 0.16–70 Hz band-pass-filtered voltage time-series were inspected for the presence of artefacts such as eye blinks, eye movements, electromyogram or muscle activity, motion effects, and electrocardiogram. EEG time segments contaminated with such patterns constituted < 10 % of any single recording. Consequently, no recordings were excluded from the study.

The effects of artefacts on subsequent quantitative analyses were minimized and signal-to-noise was maximized by an artefact-rejection data pre-processing pipeline that included an independent component analysis (ICA)-based artefact rejection scheme

[28, 29]. Bandpass filtering (0.16 Hz to 40 Hz) reduced slow drifts and high frequency artefacts with a zero phase-shift Hamming windowed-sinc FIR filter (EEGLAB function 'pop_eegfiltnew'). Then artefacts were identified and removed objectively using the ADJUST method [30]. The filtered continuous EEG data first undergoes ICA decomposition with an Extended-Infomax algorithm [31]. ADJUST then detects and removes the artefact-independent components associated with eye blinks, horizontal and vertical eye movements, and generic discontinuities. It then reconstructs a cleaned version of the original data. ▶ **Fig. 1** shows a fragment of multichannel EEG data with an eye blink artefact before and after removing the artefact by the ADJUST method.

Feature extraction

Both univariate (based on data from a single sensor) and multivariate (multiple sensors) features were used to develop methods for objectively discriminating between groups of EEGs. Pre-processed EEG was first divided into a set of adjacent, non-overlapping feature time windows of fixed size ΔT For each window, we computed the univariate frequency band-power (FBP), multivariate phase locking value (PLV), and univariate modulation index (MI) to estimate phase-amplitude coupling (PAC). These variables provide metrics to decode mental states as well as distinguish between normal and other brain activity patterns [32–34].

FBP: The frequency band power is calculated by integrating the power spectral density of EEG (within a feature time window) under a particular frequency range, then dividing it by the total power across the spectra. The magnitude of FBP estimates the local spatio-temporal synchronization of extracellular inhibitory and excitatory currents [35, 36]. Our frequency ranges were chosen in 4 Hz increments from 0 to 32 Hz, namely delta (0–4 Hz), theta (4–8 Hz), alpha (8–12 Hz), beta1 (12–16 Hz), beta2 (16–20 Hz), beta3 (20–24 Hz), beta4 (24–28 Hz), beta5 (24–28), and low gamma (28–32 Hz). The upper bound was chosen to be low gamma since cerebral activity contributes negligibly to scalp EEG beyond this range [37].

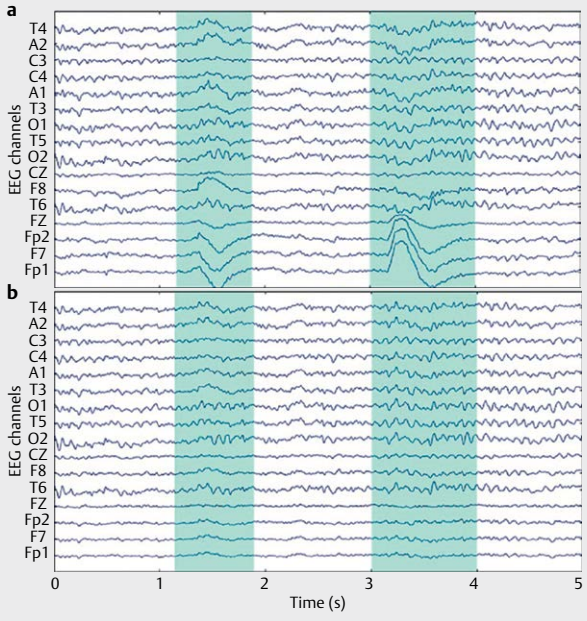

▶ **Fig. 1** The effect of artefact-detection preprocessing. A fragment of multichannel EEG data contaminated by blink artefact (**a**) before and (**b**) after the data are cleaned by the ADJUST method. The highlighted segments of the data show the effect of blinking on EEG channels.

PLV: The phase locking value (PLV) measures the phase synchronization between the narrow-band filtered EEG recorded from a pair of distinct electrodes. Accordingly, PLV quantifies long-range, frequency-specific, amplitude-independent phase synchronization of EEG oscillations between brain areas to estimate inter-area neural integration [38]. We computed PLV after filtering the EEG in 2-Hz wide bands that were centered at 4, 10, 20, and 40 Hz, which allows for precise estimates of phase [32]. The signal pairs were selected to be intra-hemispheric (F7-T5, F3-P3, F4-P4, F8-T6, FP1-O1, FP2-O2), inter-hemispheric symmetric (FP1-FP2, F7-F8, F3-F4, T3-T4, T5-T6, O1-O2), and inter-hemispheric asymmetric (FP1-O2, FP2-O1, F7-T6, F8-T5). PLV values of 1 indicate that the phase difference between the two signals is constant, whereas PLV values of zero indicate that the phase difference is uniformly distributed between 0 and 2π [33, 39]. To calculate the PLV, the pair of EEG signals were bandpass-filtered at a given frequency within a 2 Hz wide band, their phases extracted via the Hilbert transform, the phase difference, $\Delta\theta$, between the two signals was computed at every data point, and the PLV for a particular window was found as the absolute value of the mean of $\exp\{i\theta\}$ over the window [40]. (Note i=√-1.)

PAC: The phase-amplitude co-modulation estimates phase-amplitude coupling between the phase of a low frequency oscillation in the EEG and the amplitude of a high frequency oscillation, providing an estimate of local, multi-frequency organization of neuronal activity [41–43].

Following previous work, we chose the low frequency ranges theta and alpha, and high frequency ranges 15–25 Hz and 30–40 Hz. PAC was computed using the Kullback-Leibler divergence between the uniform distribution and the phase-amplitude distribution obtained from bandpass-filtered signals [44, 45].

Classification and validation

We used support vector machine (SVM) binary classification to make inferences about whether particular recordings belonged to the subgroups designated as Baseline (BL), Injury (IN), or Post-Season (PS). Since the smallest data set (IN) contained 12 recordings, we randomly selected 12 recordings from each of the BL and PS sets to have an equal number of recordings from each class. This ensured that the chance value for correct classification would be 0.5. After feature extraction the data were in the form of a matrix whose columns are different features and rows are time windows (or an observation). Every observation in our experiments has an associated label, BL, IN, or PS, thus the problem was suitable for analysis by supervised machine learning (ML). Supervised ML approaches in general, and SVM in particular, take advantage of distributed and subtle patterns of activation that are otherwise possibly undetectable, to allow inference at the level of the individual subject and specific time window, rather than at the group level.

SVM classifies data points by maximizing the margin between classes in a high-dimensional feature space (for a review and references [46]. We used SVM for pairwise binary classification.

For testing we used leave-one-out cross-validation (LOOCV). This was implemented by leaving out one observation for training the SVM, which was then tested on the left-out observation. This process was repeated for each observation. The Matlab functions svmtrain, svmclassify, and cvpartition were used to implement the above calculations. To evaluate performance, accuracy was determined as the fraction of observations that could be correctly identified in the test data.

Statistical analysis

We used statistical tests to determine the significance of our results. Specifically, we used a binomial test which calculates the p-value based on the total number of observations in each class and the chance level of accuracy [33, 47]. To test the significance of phase locking values (PLV), we created a null distribution assuming random phase differences. The p-value of PLV was calculated for each subject and time window from the null distribution. We then considered a global null hypothesis that the PLV was no better than chance for any subject and time window. We used the Bonferroni procedure to control for multiple comparisons and determined significance if p < alpha/k, where alpha was set to 0.05 and k was the total number of tests.

We chose the relatively conservative, non-parametric Kolmogorov-Smirnov (KS) test to evaluate this null hypothesis.

Results

Forty-seven EEGs were recorded from 30 distinct subjects. All EEGs were evaluated by a board-certified neurologist EEG reader and all were assessed to be technically valid and interpreted as normal, including 14 post-season EEGs, and 12 injury EEGs from 9 subjects. Three subjects contributed two injury EEGs each, and because the intervals between the two EEGs were 6, 26, and 56 days, they were treated as independent samples. None of the injury subjects had provided baseline EEGs and none provided post-season EEGs. The median duration of the EEG recordings was 21.3 minutes, with a minimum duration of 19.6 minutes and with two recordings lasting an hour or longer. It is therefore demonstrated that with the StatNet and microEEG systems, it is feasible for athletic trainers to record clinically valid resting-state EEGs from student athletes in the sports facility.

We then used machine learning to evaluate whether there were differences between the three classes of EEG. ▶ **Fig. 2** shows the values of accuracy of binary discrimination between pairs of EEG classes for feature windows of fixed size $\Delta T = 120$ s (shorter $\Delta T = 60$ s and longer $\Delta T = 240$ s feature windows did not lead to different conclusions). ▶ **Fig. 2** shows the classification results after partitioning the data in different ways. When as much of the available data are used with the limit in each class set by the class with the lowest number of EEGs (IN = 12), we find that BL and IN could be discriminated with 81 % accuracy using the FBP, PLV, and PAC EEG features together, even though discrimination based on any one feature was no better than chance. This suggests there may be a potential for additive effects, at least with small datasets such as this (▶ **Fig. 2a**). Selecting only the highest quality EEGs (N = 8 for each class) did not change the result, but now FBP and PLV measures alone were able to discriminate BL and IN better than chance, in addition to the three measures together (▶ **Fig. 2b**). Limiting one injury EEG to a subject reduced the accuracy of SVM discrimination to chance (▶ **Fig. 2c**; N = 10), unless the data set was limited to the highest quality EEGs, in which case eliminating the redundant EEGs had no effect (▶ **Fig. 2d**; N = 8). Given that BL and PS EEGs could not be discriminated using the three EEG measures together (discrimination using one measure but not all three are likely the result of overfitting and limited data) and BL and IN EEG can be discriminated, one

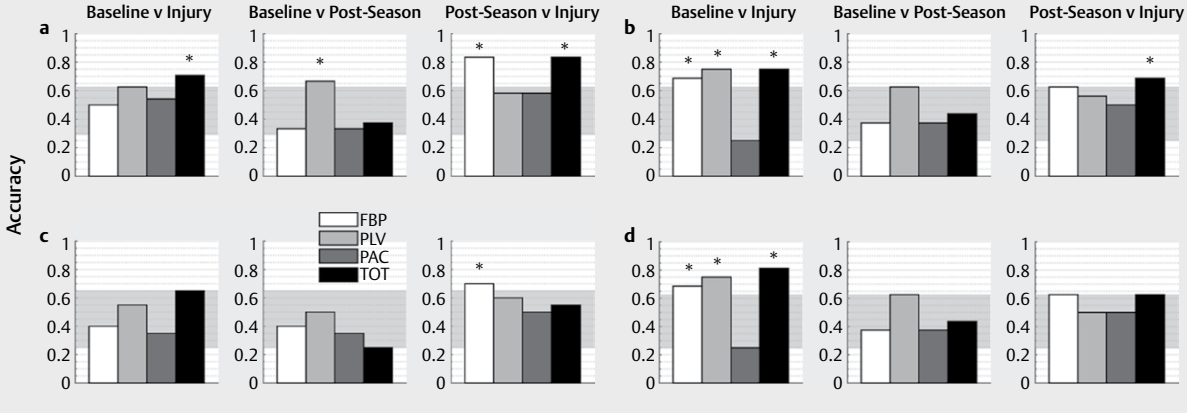

▶ **Fig. 2** Accuracy of automated binary classification of Baseline (BL) vs. Injury (IN), Baseline vs. Post-Season (PS), and PS vs. IN, with feature window size $\Delta T = 120$ s. The horizontal shaded areas in the background indicate 95 % of the null density of accuracy. (*p < 0.05.) **(a)** All available EEGs in class IN were used regardless of quality so that there were 12 recordings in every class. **(b)** EEGs were selected for quality so that there were 8 recordings in each class. Multiple recordings from subjects were allowed in (A) and (B); there were 2 such recordings, both in class IN. Decreasing quality was measured in terms of the number of segments that had been removed due to artefacts (maximum of 60 cuts being used as the quality threshold). **(c)** All available EEGs in class IN were used regardless of quality, but multiple recordings per subject were disallowed, so that there were 10 recordings in every class. **(d)** EEGs were selected for quality and multiple recordings per subject were disallowed, so that there were 8 recordings in each class.

might expect that IN and PS EEGs to also be discriminable. However as shown in ▶ **Fig. 2**, this was not reliably the case. Although the pattern of results presented ▶ **Fig. 2** demonstrates the possibility of successfully discriminating BL and IN EEGs, the inability to discriminate PS and IN EEGs, as well as BL and PS, indicates there are non-linear complexities in using the SVM approach, likely due to the small data set, and sensitivity to artefacts in the EEGs.

Having examined the classification accuracy of various feature types, we investigated the spatiotemporal patterns in the values of the various types of features in the different EEG classes BL, IN, and PS.

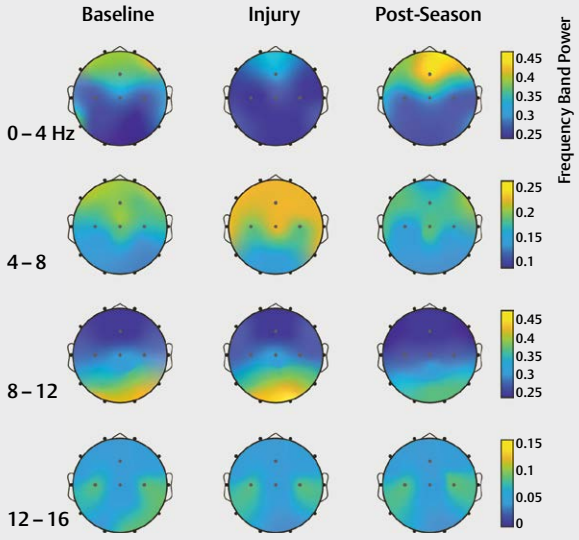

▶ **Fig. 3** Topographic distribution of frequency band power ΔT = 60 s. Electrode locations are indicated by small grey dots. The values shown (color bar at right) represent averages over the entire set of recordings in the class BL (left column), IN (middle), or PS (right).

▶ **Fig. 2** suggested that FBP may differ significantly between the baseline and injured subjects. ▶ **Fig. 3** compares the topographic distribution of this feature for the delta to alpha frequency ranges. The figure indicates clear differences in the distribution of delta, theta, and alpha power between the BL and IN groups. Meanwhile the BL and PS groups appear to differ, to a smaller extent, only in alpha power distribution. Overall, the IN EEGs appear to express reduced frontal delta and increased frontal theta, providing a basis for SVM discriminations.

To further investigate this hypothesis, we considered the channel-averaged FBP in the different frequency ranges in ▶ **Fig. 4a**. Overall delta, theta, and alpha power do not appear different in the three groups of EEG, not only is the inter-subject variability large, but as can be seen in ▶ **Fig. 4**, the abnormal power is not homogeneously distributed across the scalp and thus not measurable as a spatial average. We nonetheless examined whether combinations of power in various frequency bands could provide a succinct discriminator of non-injured and injured EEGs. To visualize this possibility, we show in ▶ **Fig. 4b** the recordings as a scatter plot in the plane of Theta/Gamma (x-axis) and Alpha/Delta power (y-axis). The figure indicates that injured subjects may have greater values of these two composite variables, relative to the BL and PS recordings, which appear to be mostly lumped together close to the origin. However, although the regions occupied by the IN versus other classes of recordings are somewhat distinct, they are not disjointed and there is substantial overlap.

▶ **Fig. 2** highlighted PLV as an important discriminator of IN, suggesting that frequency-specific inter-area synchrony may be altered in injured subjects. We now investigate the specific frequencies and pairs of sites that may differentially contribute to this result. ▶ **Fig. 2** shows PLV calculated for 4 Hz (top row), 10 Hz (2nd row), 20 Hz (3rd row), and 30 Hz (bottom row). The error bars show the standard deviation of intersubject variability. Values of PLV differing significantly between any pair of groups are indicated by an asterisk above the pair of bars (*$p < 0.05$.). The figure clearly flags mostly frontal inter-hemispheric connectivity as an important discriminator of the IN state, since most of the significantly differing

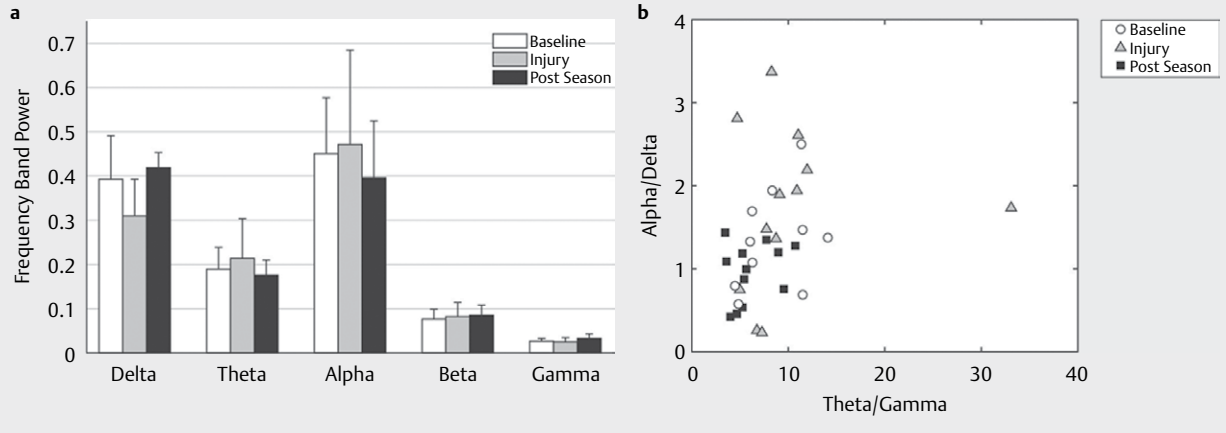

▶ **Fig. 4** Indicators derived from time averaged band power in standard ranges of frequency. **a**: Error bars indicate the standard deviation of intersubject variability within the same class (BL, IN, or PS). **b**: Time averaged FBP shown in the plane of Theta/Gamma (x-axis) and Alpha/Delta power (y-axis). Each point represents a distinct recording in the class BL (circle), IN (triangle), and PS (square).

PLV values occur in pairs that symmetrically connect the frontal hemispheres (FP1-FP2, F7-F8, and T3-T4).

Additional details are provided in ▶ **Table 1**, which displays the PLV at multiple frequencies and locations. The value of the PLV is provided for the Baseline, Injury, and Post-Season states. Each one of these PLVs is statistically significant in accordance with the Bonferroni corrected procedure described in the Methods section. To the right of the three PLV columns, an additional three columns show whether the differences in PLV between IN and BL, PS and IN, and PS and BL were statistically significant. The table includes only frequencies and locations for which at least one of these differences was significant. Significance was calculated by a non-parametric method explained in the Methods section. It is indicated by an asterisk in the table. The differences are also color-coded, so that red indicates a positive and blue a negative difference. For example, if the PLV for injured recordings was lower than baseline, then the table entry under IN-BL is blue.

The table shows that PLV of injured subjects was generally lower than baseline in the lower frequencies (up to low gamma range) in some frontal inter-hemispheric electrode pairs (blue squares in column titled IN-BL). They were also lower than the PLV measured post-season (red squares in column titled PS-IN). In addition, the table indicates that in these frequencies and pairs of sites, post-season PLV was lower than baseline (blue squares in column titled PS-BL).

▶ **Table 1** Phase locking value (PLV) for the Baseline (BL), Injury (IN), and Post-Season (PS) averaged over subjects, and the statistical significance (*$p > 0.05$) and positive/negative (red/blue) in difference in the PLV of two states. The most available quality-selected data (N = 8, as in ▶ **Fig. 2b**) were used for these comparisons.

To visualize the changes in functional connectivity implied by the values in ▶ **Table 1** and ▶ **Fig. 5**, we plot each statistically significant PLV difference as a line that connects the corresponding pair of electrodes in ▶ **Fig. 6**. The figure shows that PLV changes are associated mostly with the inter-hemispheric pair F7-F8 in the delta, alpha, and beta frequencies, while they are also associated with intra-hemispheric connections centering on F8 in the low-gamma frequencies.

Discussion and conclusions

This paper addressed the diagnosis of mTBI, a public health concern affecting a very large population including children, athletes, and military personnel. The study was designed as a proof-of-principle feasibility trial, importantly without an independent control group. Nonetheless, this design yielded results demonstrating that it is feasible for athletic trainers at a sports facility to record clinically valid, high-quality resting-state EEGs from student athletes. The findings also show that spatially-localized metrics of EEG synchrony can discriminate mTBI-associated EEGs from control EEGs. These findings provide proof-of-concept evidence that resting-state EEG is a practical, non-invasive measurement technique that

▶ **Table 1** Phase locking value (PLV) for the Baseline (BL), Injury (IN), and Post-Season (PS) averaged over subjects.

Frequency (Hz)	Electrode Pairs	PLV			PLV Difference		
		Baseline (BL)	Injury (IN)	Post-Season (PS)	IN-BL	PS-IN	PS-BL
4	FP1-FP2	0.758	0.66	0.614	*		*
	F7-F8	0.854	0.754	0.863	*	*	
	T3-T4	0.578	0.485	0.586		*	
10	FP1-FP2	0.821	0.795	0.728		*	*
	F7-F8	0.81	0.715	0.823	*	*	
15	FP1-O1	0.275	0.24	0.279		*	
	FP1-FP2	0.757	0.628	0.595			*
	F7-F8	0.789	0.685	0.811		*	
	FP1-O2	0.223	0.195	0.251		*	
20	FP1-FP2	0.732	0.619	0.567			*
	F7-F8	0.791	0.724	0.815	*		
25	FP1-FP2	0.712	0.562	0.513			*
	F7-F8	0.79	0.732	0.816	*		
30	F8-T6	0.325	0.375	0.365	*		
	FP1-FP2	0.703	0.498	0.45			*
	F7-F8	0.787	0.716	0.811	*		
	F8-T5	0.271	0.36	0.328	*		
35	F8-T6	0.289	0.329	0.325	*		*
	FP1-FP2	0.69	0.452	0.403			*
	F7-F8	0.779	0.701	0.802	*		*
	F8-T5	0.235	0.322	0.291	*		
40	FP1-FP2	0.687	0.448	0.407			*
	F7-F8	0.777	0.706	0.804	*		
	F8-T5	0.232	0.331	0.294	*		

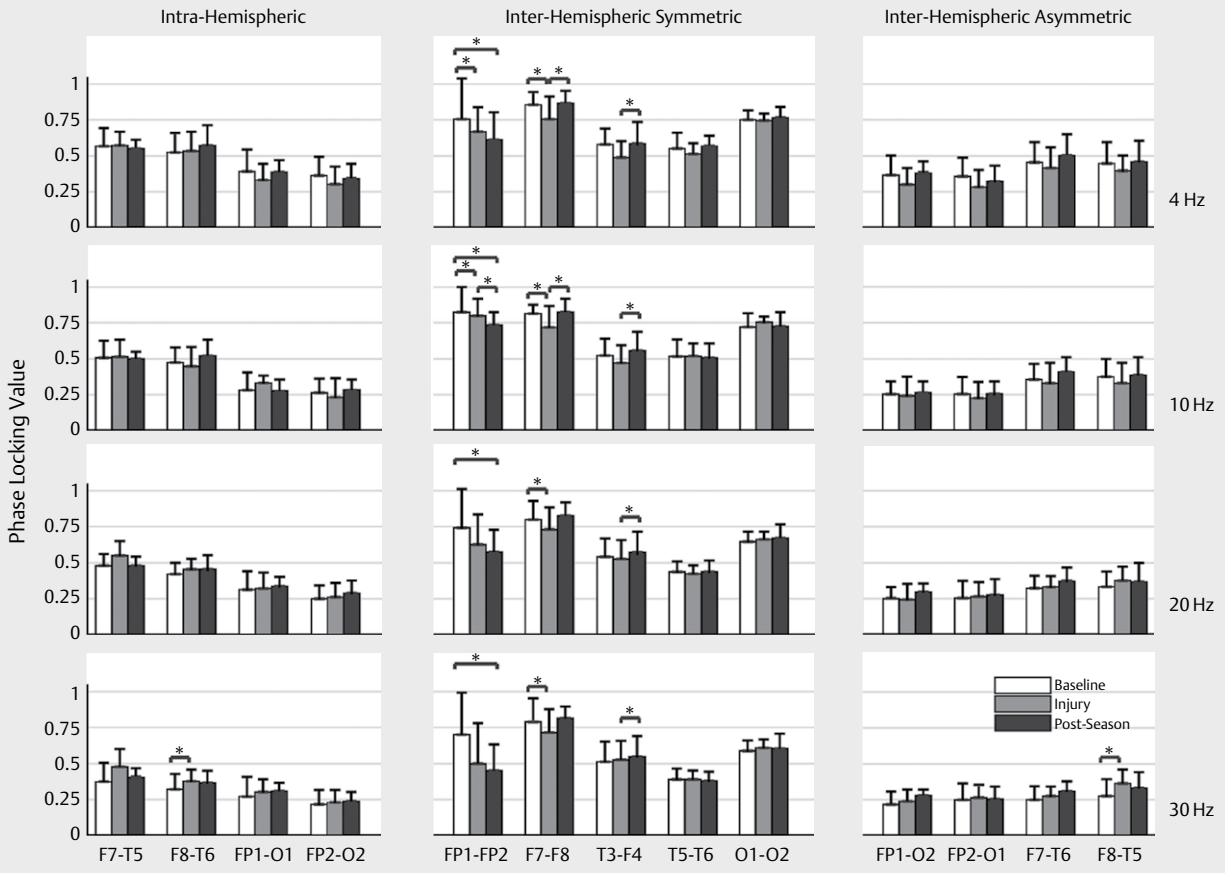

▶ **Fig. 5** PLV at multiple frequencies and pairs of electrodes. The error bars indicate the standard deviation of intersubject variability. (*$p<0.05$)

can be implemented by minimally trained personnel to help diagnose mTBI. Performing on-site head trauma screening or assessment on the sidelines is preferred for timely evaluation and decision-making. This approach is particularly important for mild injuries where symptoms may not be immediately apparent and there is a risk of second impact syndrome.

There were differences among the Baseline, Injury, and Post-Season EEGs in the frequency band power features, which estimates the degree of synchronized synaptic currents local to the electrode site, effects of volume conduction notwithstanding. Reduced delta and increased theta at frontal sites characterized injury EEGs, with only a weak tendency to increased alpha at posterior sites (▶ **Fig. 3**). With respect to the Baseline EEGs, the Injury EEGs had higher theta and lower delta power. Interestingly, relative to Baseline EEGs, we also found that the Post-Season EEGs had frequency-band- and location-specific changes that were in the opposite direction as the injury-associated EEGs. Such alterations were sufficient for 25 % above chance accuracy of classifying Baseline and Injury EEGs (▶ **Fig. 2**). While the observed power differences were relatively specific, they did not differentiate between the EEGs of the Baseline and Post-Season groups. This is not unexpected, as both groups were comprised of athletes without head injuries and were anticipated to have comparable features. Furthermore, these power differences were also insufficient to distinguish between the EEGs of the Injury and Post-Season groups.

In contrast, we found no systematic EEG class differences in estimates of PAC computed locally, i. e., at single electrode sites. It is worth noting that inter-area PAC based on resting-state magnetoencephalography of mTBI patients was found to differ between mTBI patients and controls, suggesting that mTBI might affect measures of inter-areal neural synchronization, which depend on the coordination of long-range conduction velocities and delays that are mediated in part by the integrity of myelination [48].

Consistent with inter-areal disturbances in mTBI, prominent differences among the three EEG classes were found in the phase locking index that estimates the degree of frequency-specific phase synchronization between distinct brain areas. Although we calculated PLV for multiple pairs of sites, the statistically significant injury-associated alterations were found mostly in inter-hemispheric symmetric sites at frontal electrodes and mid-line (▶ **Fig. 6**). These are populations located on either side of and equally distant from the midline sagittal plane, such as the left and right orbitofrontal sites FP1 and FP2. The inter-group changes were particularly strong at 4 and 10 Hz, which are EEG oscillation frequencies known to have non-local biophysical origins, unlike gamma, which is generated locally [49]. As in the case of FBP, these differences are

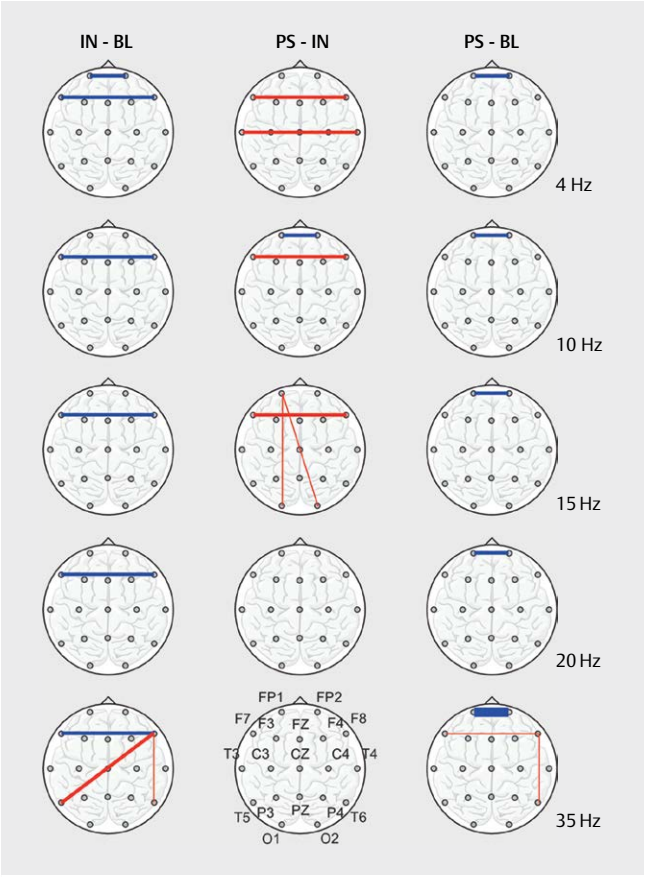

▶ **Fig. 6** The difference in PLV between subject states visualized across multiple pairs of topographic sites and frequencies. The thickness of the line connecting a pair of electrodes is linearly proportional to the absolute value of the PLV change. As in ▶ **Table 1**, positive (negative) differences are shown in red (blue). Only PLV changes that are significantly above chance are shown.

sufficient for a 25 % greater than chance accuracy of classifying Baseline and Injury EEGs (▶ **Fig. 2**).

Thus, the present findings are consistent with reduced interhemispheric synchrony that can be attributed to changes in white matter microstructure, including weakened alpha frequency interhemispheric synchrony that can be detected by resting state magnetoencephalography of mTBI patients [34, 50–52].

mTBI patients often suffer from problems in attention, memory, and executive function, all high-level functions enabled by multiple brain regions integrated by long-range connections [53]. Electrographic findings from mTBI patients include slowing and reduced alpha activity and such findings within the first 24 h have been associated with worse recovery, however traditional EEG interpretation needs to be enhanced by quantitative analysis to reveal changes to functional connectivity, as suggested by the present findings [54].

Thus, our findings, though preliminary, are nonetheless consistent with the reduced inter-hemispheric functional connectivity that was reported in a fMRI study of athletes with mTBI at 10 days after injury [50]. Resting-state fMRI of mTBI patients also showed reduced connectivity in the default mode network pattern in the days and weeks following injury [49, 55, 56].

Despite its advantages in superior spatial resolution, the expense and lack of portability make fMRI largely unsuitable for many applications, whereas as demonstrated here, resting-state EEG with portable and easy-to-deploy equipment may be convenient, feasible, and similarly effective to screen for mTBI and for evaluating return-to play decisions.

Our results may form the basis for a rapid and practical method to diagnose mTBI in the clinic as well as in the field but additional, controlled studies with independent injury and control groups will be important for validating this possibility. Better diagnosis of mTBI would not only help in the management of athletes but also help increase the efficiency of clinical trials through methods suitable for identifying a cohort of mTBI patients at higher risk of developing long-term problems [57]. The study represents a step towards increasing access to brain injury care and reducing inequity in various settings, including the military, and athletic facilities. This approach has the potential to contribute to the development of more effective and accessible tools for the detection of mild traumatic brain injuries, with broad implications for the improvement of functional outcomes and quality of life of those affected.

The ability to identify patients at high risk of long-term problems would help to appropriately channel scarce clinical resources such as specialty follow-up and rehabilitation. Clinical trials are likely to be enriched if they recruit patients with a high probability of brain dysfunctions post-injury.

Acknowledgements

We thank the following MIT representatives for their expertise and assistance throughout all aspects of our study: For her role as on-campus Principle Investigator, Associate Professor/Head Coach Women's Tennis; Carol Matsuzaki. For their roles as Associate Investigators: Dr. Shawn Ferullo, Dr. Angelene Elliott, Jessica Rooney Gallagher, ATC, and Thomas Cronan, ATC.

Conflict of Interest

The authors have disclosed conflicts of interest, which are as follows: Bio-Signal Group Corporation loaned and/or paid for the needed equipment. Dr. Samah G. Abdul Baki reports support from Bio-Signal Group Corporation and other grants outside the submitted work. In addition, Dr. Baki has a patent 61/554,743 pending and a U.S. patent 13/284,886. Dr. André Fenton is the esteemed founder of Bio-Signal Group Corporation, in which he holds an equity interest. It is worth noting that he has not derived any financial benefits from this involvement thus far. Dr Ahmet Omurtag worked for Bio-Signal Group Corporation in 2008-2013, which makes the device used in this study. At the time he was given stocks of the company. Since the company is not public, their value was theoretical only. We are not sure what the potential value (if any) might be at the moment.

References

[1] Menon DK, Schwab K, Wright DW et al. Position statement: definition of traumatic brain injury. Arch Phys Med Rehabil 2010; 91: 1637–1640

[2] Coronado VG, McGuire LC, Sarmiento K et al. Trends in traumatic brain injury in the US and the public health response: 1995–2009. J Safety Res 2012; 43: 299–307

[3] Kay T, Harrington DE, Adams R. American congress of rehabilitation medicine, head injury interdisciplinary special interest group. definition of mild traumatic brain injury. J Head Trauma Rehabil 1993; 8: 86–87

[4] McMahon PJ, Hricik A, Yue JK et al. Symptomatology and functional outcome in mild traumatic brain injury: results from the prospective TRACK-TBI study. J Neurotrauma 2014; 31: 26–33

[5] Levin HS, Diaz-Arrastia RR. Diagnosis, prognosis, and clinical management of mild traumatic brain injury. Lancet Neurol 2015; 14: 506–517

[6] Iverson GL, Langlois JA, McCrea MA et al. Challenges associated with post-deployment screening for mild traumatic brain injury in military personnel. Clin Neuropsychol 2009; 23: 1299–1314

[7] Jacobs B, Beems T, Stulemeijer M et al. Outcome prediction in mild traumatic brain injury: age and clinical variables are stronger predictors than CT abnormalities. J Neurotrauma 2010; 27: 655–668

[8] Lannsjö M, Backheden M, Johansson U et al. Does head CT scan pathology predict outcome after mild traumatic brain injury? Eur J Neurol 2013; 20: 124–129

[9] Shenton ME, Hamoda HM, Schneiderman JS et al. A review of magnetic resonance imaging and diffusion tensor imaging findings in mild traumatic brain injury. Brain Imaging Behav 2012; 6: 137–192

[10] Belanger HG, Vanderploeg RD, Curtiss G et al. Recent neuroimaging techniques in mild traumatic brain injury. J Neuropsychiatry Clin Neurosci 2007; 19: 5–20

[11] Levin HS, Wilde E, Troyanskaya M et al. Diffusion tensor imaging of mild to moderate blast-related traumatic brain injury and its sequelae. J Neurotrauma 2010; 27: 683–694

[12] Leh SE, Schroeder C, Chen J-K et al. Microstructural integrity of hippocampal subregions is impaired after mild traumatic brain injury. J Neurotrauma 2017; 34: 1402–1411

[13] Bazarian JJ, McClung J, Cheng YT et al. Emergency department management of mild traumatic brain injury in the USA. Emerg Med J 2005; 22: 473–477

[14] Faul M, Xu L, Wald MM et al. Traumatic brain injury in the United States: Emergency Department Visits, Hospitalizations and Deaths 2002–2006. Atlanta GA: Cent Dis Control Prev Natl Cent Inj Prev Control; 2010

[15] Laskowski RA, Creed JA, Raghupathi R. Pathophysiology of mild TBI: implications for altered signaling pathways. In: Kobeissy FH, ed. brain neurotrauma: molecular, neuropsychological, and rehabilitation aspects. Boca Raton (FL): CRC Press/Taylor & Francis; 2015

[16] Shin SS, Bales JW, Dixon CE et al. Structural imaging of mild traumatic brain injury may not be enough: overview of functional and metabolic imaging of mild traumatic brain injury. Brain Imaging Behav 2017; 11: 591–610

[17] Meier B, Ivory D. Effective concussion treatment remains frustratingly elusive, despite a booming industry. Available from: https://www.nytimes.com/2015/07/05/business/effective-concussion-treatment-remains-frustratingly-elusive-despite-a-booming-industry.html

[18] Abbas K, Shenk TE, Poole VN et al. Alteration of default mode network in high school football athletes due to repetitive subconcussive mild traumatic brain injury: a resting-state functional magnetic resonance imaging study. Brain Connect 2015; 5: 91–101

[19] Zhu DC, Covassin T, Nogle S et al. A potential biomarker in sports-related concussion: brain functional connectivity alteration of the default-mode network measured with longitudinal resting-state fMRI over thirty days. J Neurotrauma 2015; 32: 327–341

[20] Coughlin JM, Wang Y, Munro CA et al. Neuroinflammation and brain atrophy in former NFL players: an in vivo multimodal imaging pilot study. Neurobiol Dis 2015; 74: 58–65

[21] Bailes JE, Petraglia AL, Omalu BI et al. Role of subconcussion in repetitive mild traumatic brain injury. J Neurosurg 2013; 119: 1235–1245

[22] Barr WB, Prichep LS, Chabot R et al. Measuring brain electrical activity to track recovery from sport-related concussion. Brain Inj 2012; 26: 58–66

[23] McCrea M, Prichep L, Powell MR et al. Acute effects and recovery after sport-related concussion: a neurocognitive and quantitative brain electrical activity study. J Head Trauma Rehabil 2010; 25: 283–292

[24] Harriss DJ, MacSween A, Atkinson G. Ethical standards in sport and exercise science research: 2020 update. Int J Sports Med 2019; 40: 813–817

[25] Ladino LD, Voll A, Dash D et al. StatNet Electroencephalogram: A fast and reliable option to diagnose nonconvulsive status epilepticus in emergency setting. Can J Neurol Sci 2016; 43: 254–260

[26] Grant AC, Abdel-Baki SG, Omurtag A et al. Diagnostic accuracy of microEEG: a miniature, wireless EEG device. Epilepsy Behav 2014; 34: 81–85

[27] Omurtag A, Baki SGA, Chari G et al. Technical and clinical analysis of microEEG: a miniature wireless EEG device designed to record high-quality EEG in the emergency department. Int J Emerg Med 2012; 5: 35

[28] Zakeri Z. Optimised use of independent component analysis for EEG signal processing. PhD Thesis. University of Birmingham 2017

[29] Zakeri Z, Assecondi S, Bagshaw AP et al. Influence of signal preprocessing on ICA-based EEG decomposition. In: XIII Mediterranean Conference on Medical and Biological Engineering and Computing 2013. IFMBE Proceedings, vol. 41. Cham: Springer. DOI: 10.1007/978-3-319-00846-2_182

[30] Mognon A, Jovicich J, Bruzzone L et al. ADJUST: An automatic EEG artifact detector based on the joint use of spatial and temporal features. Psychophysiology 2011; 48: 229–240

[31] Lee T-W, Girolami M, Sejnowski TJ. Independent component analysis using an extended infomax algorithm for mixed subgaussian and supergaussian sources. Neural Comput 1999; 11: 417–441

[32] Dvorak D, Fenton AA. Toward a proper estimation of phase–amplitude coupling in neural oscillations. J Neurosci Methods 2014; 225: 42–56

[33] Omurtag A, Aghajani H, Keles HO. Decoding human mental states by whole-head EEG + fNIRS during category fluency task performance. J Neural Eng 2017; 14: 066003

[34] Vakorin VA, Doesburg SM, da Costa L et al. Detecting mild traumatic brain injury using resting state magnetoencephalographic connectivity. PLoS Comput Biol 2016; 12: e1004914

[35] Buzsáki G, Anastassiou CA, Koch C. The origin of extracellular fields and currents—EEG, ECoG, LFP and spikes. Nat Rev Neurosci 2012; 13: 407

[36] Gevins A, Smith ME. Neurophysiological measures of working memory and individual differences in cognitive ability and cognitive style. Cereb Cortex 2000; 829–839

[37] Petroff OA, Spencer DD. Goncharova II et al. A comparison of the power spectral density of scalp EEG and subjacent electrocorticograms. Clin Neurophysiol 2016; 127: 1108–1112

[38] Varela F, Lachaux J-P, Rodriguez E et al. The brainweb: phase synchronization and large-scale integration. Nat Rev Neurosci 2001; 2: 229–239

[39] Lachaux J-P, Rodriguez E, Martinerie J et al. Measuring phase synchrony in brain signals. Hum Brain Mapp 1999; 8: 194–208

[40] Le Van Quyen M, Foucher J, Lachaux J-P et al. Comparison of Hilbert transform and wavelet methods for the analysis of neuronal synchrony. J Neurosci Methods 2001; 111: 83–98

[41] Aghajani H, Garbey M, Omurtag A. Measuring mental workload with EEG + fNIRS. Front Hum Neurosci 2017; 11: 359

[42] Canolty RT, Edwards E, Dalal SS et al. High gamma power is phase-locked to theta oscillations in human neocortex. Science 2006; 313: 1626–1628

[43] Radwan B, Dvorak D, Fenton AA. Impaired cognitive discrimination and discoordination of coupled theta–gamma oscillations in Fmr1 knockout mice. Neurobiol Dis 2016; 88: 125–138

[44] Dvorak D, Shang A, Abdel-Baki S et al. Cognitive behavior classification from scalp EEG signals. IEEE Trans Neural Syst Rehabil Eng 2018; 26: 729–739

[45] Tort AB, Komorowski R, Eichenbaum H et al. Measuring phase-amplitude coupling between neuronal oscillations of different frequencies. J Neurophysiol 2010; 104: 1195–1210

[46] Orrù G, Pettersson-Yeo W, Marquand AF et al. Using support vector machine to identify imaging biomarkers of neurological and psychiatric disease: a critical review. Neurosci Biobehav Rev 2012; 36: 1140–1152

[47] Combrisson E, Jerbi K. Exceeding chance level by chance: The caveat of theoretical chance levels in brain signal classification and statistical assessment of decoding accuracy. J Neurosci Methods 2015; 250: 126–136

[48] Antonakakis M, Dimitriadis SI, Zervakis M et al. Altered cross-frequency coupling in resting-state MEG after mild traumatic brain injury. Int J Psychophysiol 2016; 102: 1–11

[49] Mayer AR, Mannell MV, Ling J et al. Functional connectivity in mild traumatic brain injury. Hum Brain Mapp 2011; 32: 1825–1835

[50] Cao C, Slobounov S. Alteration of cortical functional connectivity as a result of traumatic brain injury revealed by graph theory, ICA, and sLORETA analyses of EEG signals. IEEE Trans Neural Syst Rehabil Eng 2010; 18: 11–19

[51] Sponheim SR, McGuire KA, Kang SS et al. Evidence of disrupted functional connectivity in the brain after combat-related blast injury. Neuroimage 2011; 54: S21–S29

[52] Tarapore PE, Findlay AM, LaHue SC et al. Resting state magnetoencephalography functional connectivity in traumatic brain injury. J Neurosurg 2013; 118: 1306–1316

[53] Kinnunen KM, Greenwood R, Powell JH et al. White matter damage and cognitive impairment after traumatic brain injury. Brain J Neurol 2011; 134: 449–463

[54] Hessen E, Nestvold K. Indicators of complicated mild TBI predict MMPI-2 scores after 23 years. Brain Inj 2009; 23: 234–242

[55] Iraji A, Benson RR, Welch RD et al. Resting state functional connectivity in mild traumatic brain injury at the acute stage: independent component and seed-based analyses. J Neurotrauma 2015; 32: 1031–1045

[56] Zhou Y, Milham MP, Lui YW et al. Default-mode network disruption in mild traumatic brain injury. Radiology 2012; 265: 882–892

[57] Ratcliff JJ, Adeoye O, Lindsell CJ et al. ED disposition of the Glasgow Coma Scale 13 to 15 traumatic brain injury patient: analysis of the Transforming Research and Clinical Knowledge in TBI study. Am J Emerg Med 2014; 32: 844–850